Brazilian Journal of Physics
ISSN: 0103-9733
luizno.bjp@gmail.com
Sociedade Brasileira de Física
Brasil

Luiz, F. S.; Duzzioni, E. I.; Sanz, L.
Implementation of Quantum Logic Gates Using Coupled Bose-Einstein Condensates
Brazilian Journal of Physics, vol. 45, núm. 5, 2015, pp. 550-559
Sociedade Brasileira de Física
São Paulo, Brasil

Available in: http://www.redalyc.org/articulo.oa?id=46442559008

How to cite
Complete issue
More information about this article
Journal's homepage in redalyc.org

Scientific Information System
Network of Scientific Journals from Latin America, the Caribbean, Spain and Portugal
Non-profit academic project, developed under the open access initiative

Braz J Phys (2015) 45:550–559
DOI 10.1007/s13538-015-0347-6

SOCIEDADE BRASILEIRA DE FÍSICA

ATOMIC PHYSICS

Implementation of Quantum Logic Gates Using Coupled Bose-Einstein Condensates

F. S. Luiz[1,3] · E. I. Duzzioni[2] · L. Sanz[1]

Received: 28 April 2015 / Published online: 15 August 2015
© Sociedade Brasileira de Física 2015

Abstract In this work, we are interested in the implementation of single-qubit gates on coupled Bose-Einstein condensates (BECs). The system, a feasible candidate for a qubit, consists of condensed atoms in different hyperfine levels coupled by a two-photon transition. It is well established that the dynamics of coupled BECs can be described by the two-mode Hamiltonian that takes into account the confinement potential of the trap and the effects of collisions associated with each condensate. Other effects, such as collisions between atoms belonging to different BECs and detuning, are included in this approach. We demonstrate how to implement two types of quantum logic gates: *population-transfer* gates (NOT, $\hat{Y}$, and Hadamard), which require a population inversion between hyperfine levels, and *phase* gates ($\hat{Z}$, $\hat{S}$, and $\hat{T}$), which require self-trapping. We also discuss the experimental feasibility by evaluating the robustness of quantum gates against variations of physical parameters outside of the ideal conditions for the implementation of each quantum logic gate.

Keywords Bose-Einstein condensates · Quantum information · Quantum logic gates

✉ L. Sanz
lsanz@infis.ufu.br

[1] Instituto de Física, Universidade Federal de Uberlândia, 38400-902, Uberlândia, MG, Brazil

[2] Departamento de Física, Universidade Federal de Santa Catarina, 88040-900, Florianópolis, SC, Brazil

[3] Present address: Departamento de Física, Universidade Federal de São Carlos, São Carlos, SP, Brazil

1 Introduction

Quantum information processing (QIP) has been one of the remarkable research topics in the field of physics over the past decades [25, 28]. Polynomial versus superpolynomial times in factorization and faster search algorithms [18, 34] are two examples of the advantages of this type of processing. The first requirement for the implementation of QIP is defining a quantum of information or qubit [33], which can be achieved using a two-level physical system. In addition, to associate the logic states 0 and 1 with one of two levels, the dynamics of the system should allow the preparation of superpositions of these states, which must be robust against decoherence. Several systems have been reported to be good candidates for the implementation of a qubit. These systems include photons, ions, charges, and spins in semiconductor nanostructures, Josephson junctions of superconductors, nuclear spins, and trapped neutral atoms [25].

Once a qubit is defined, certain physical requirements for the implementation of QIP must be fulfilled [25]. One such requirement is the existence of a universal logic, which guarantees the manipulation of the information contained in the qubit. In mathematical terms, quantum states can be represented as vectors that are transformed by operators, represented as matrices. These operators are known as *quantum logic gates*. It is of fundamental importance to explore how to implement this unitary operation to obtain a set of universal quantum gates. One example is the set formed by the single-qubit Hadamard and phase gates, together with the two-qubit CNOT gate.

Regarding trapped atoms, Bose-Einstein condensates (BECs) with alkali atoms, which were created in 1995 [2, 12], have been reported to be promising candidates for the implementation of QIP proposals because of the long decoherence time scale and the high degree of manipulation, as

well as the control over their physical properties. In particular, coupled Bose-Einstein condensates (CBECs) can be implemented using two experimental setups. In the first, atoms condensed in two different sites of an optical lattice are coupled by tunneling [9, 32]. The second configuration consists of condensed atoms in different hyperfine levels coupled by a laser [19, 20]. The two-mode model provides an adequate theoretical description of the dynamics of both systems [27]. Experimental achievements on coupled BECs include the observation of coherent oscillations [1, 9, 20], the realization of coupled condensates inside a chip [4, 21], the creation of atomic interferometers [17], and entangled quantum states [16]. Because the process of population transfer is performed with high quality in a fully controlled experimental setup, the system can be considered, to a first approximation, in an equilibrium state. However, the effect of the presence of non-condensed atoms over the coupled condensate is one of the causes behind the destruction of the condensate, and the time scales are long enough for QIP operations.

There are a few theoretical proposals for the implementation of gates in coupled BECs. These include the works of Calarco et al. [6, 7], which focused on analyzing the conditions for implementing a phase gate by manipulating confinement potentials and quantum logic gates using marker atoms [8]. Pachos and Knight [29] proposed two-qubit operations, including a Toffoli gate, by combining both tunneling and adiabatic passage of condensate atoms in a superlattice. Lee et al. explored the dipole-dipole interaction as a coupling mechanism [26]. In a recent work, Byrnes et al. [5] proposed the codification of a quantum bit by using an atomic coherent state, as well as the implementation of the two-qubit CNOT gate and an application to Grover's algorithm [18]. The authors noted that this proposal possesses a natural advantage as the energy scale of the interaction is enhanced by a factor corresponding to the number of condensed atoms, with the consequence of reducing the time of the CNOT gate by the same factor. Regarding single-qubit operations, it was discussed how to rotate the qubit around z. Regardless, there is a lack of information about the practical implementation of single-qubit quantum logic gates.

In this work, we explore the dynamics of coupled BECs and demonstrate how to implement *controlled* single-qubit quantum logic gates. Our physical system consists of atoms in a magneto-optical trap, condensed in two different hyperfine levels that are coupled by a two-photon transition. First, we obtain an analytical solution for the time-dependent Schrödinger equation, written as an evolution operator. Then, we demonstrate that dynamics can be rewritten as successive applications of rotation operators, $\hat{R}_i$. Finally, we explore this general result to determine the conditions over the physical parameters that control the dynamics of the system in such a way that corresponds to the action of six quantum logic operations: the gates NOT, Y, and Hadamard, which require a population transfer, and the phase gates $\hat{Z}$ (π), $\hat{S}$ $(\pi/2)$, and $\hat{T}$ $(\pi/4)$, which require the inhibition of the population transfer using strong detuning.

The remainder of this paper is organized as follows: in Section 2, we obtain an analytical solution for the evolution operator associated with the two-mode Hamiltonian, following a procedure similar to that used in a previous work [14]. In Section 3, we determine the physical conditions for the implementation of the six quantum logic gates, while in Section 4, we discuss the experimental feasibility of our proposal. In Section 5, we summarize our results.

2 Dynamics of Coupled BECs

Our system consists of condensed atoms in two different hyperfine levels, which are labeled as a and b. The interactions between the atoms are well described by assuming two-body collisions, and the coupling of the two hyperfine levels is achieved via a two-photon transition. The second-quantized Hamiltonian is written as ($\hbar = 1$) [11, 27, 35, 37]

$$\hat{H} = \tilde{\omega}_a \hat{n}_a + \tilde{\omega}_b \hat{n}_b + \gamma_a \hat{n}_a^2 + \gamma_b \hat{n}_b^2 + 2\gamma_{ab} \hat{n}_a \hat{n}_b - g\left(\hat{a}^\dagger \hat{b} e^{-\imath \Delta t} + \hat{a}\hat{b}^\dagger e^{\imath \Delta t}\right), \quad (1)$$

where $\hat{a}$ and $\hat{b}$ are bosonic operators for each condensate, $\hat{n}_a = \hat{a}^\dagger \hat{a}$, $\hat{n}_b = \hat{b}^\dagger \hat{b}$, and we define the following physical parameters

$$\omega_j = \int d^3\vec{r} \Phi_j(\vec{r}) \left[-\frac{1}{2m}\nabla^2 + V_j(\vec{r})\right] \Phi_j(\vec{r}), \quad (2)$$

$$\gamma_j = \frac{4\pi A_j}{2m} \int d^3\vec{r} \Psi_j^4(\vec{r}),$$

$$\gamma_{ab} = \frac{4\pi A_{ab}}{2m} \int d^3\vec{r} \Psi_a^2(\vec{r}) \Psi_b^2(\vec{r}),$$

$$g = \frac{\Omega}{2} \int d^3\vec{r} \Psi_a(\vec{r}) \Psi_b(\vec{r}).$$

Here ($j = a,b$), ω_j describes the effect of a harmonic potential over the condensed atoms; γ_j depends on the scattering length A_j, describing collisions between the atoms condensed in the same hyperfine level a or b; and γ_{ab} is associated with the collisions between atoms in different levels. The coupling parameter g takes into account the effect of a two-photon coupling between two different hyperfine levels, with Ω being the coupling strength between the modes. This coupling could be resonant ($\Delta = 0$) or not ($\Delta \neq 0$). In (1), we also use the auxiliary parameters $\tilde{\omega}_{(a,b)} = \omega_{(a,b)} - \gamma_{(a,b)}$.

The task here is to find the evolution operator $\hat{P}(t)$ that evolves some initial state. The evolved state, which is the solution of the Schrödinger equation associated with Hamiltonian (1), can be written as

$$|\Psi(t)\rangle = \hat{P}(t)\,|\Psi(0)\rangle. \quad (3)$$

To find $\hat{P}(t)$, we use a technique that takes advantage of the properties of unitary transformations. We successively apply two transformations, where the first one is

$$\hat{U}(t) = e^{\frac{-\iota\Delta t}{2}(\hat{n}_a - \hat{n}_b)},$$

which removes the explicit temporal dependence from the original Hamiltonian (1). After the application of $\hat{U}(t)$, the evolved state (3) reads as

$$|\Psi(t)\rangle = \hat{U}(t)\left|\Psi^U(t)\right\rangle,$$

where the transformed state $\left|\Psi^U(t)\right\rangle$ is the solution of the Schrödinger equation associated with the transformed Hamiltonian $\hat{H}^U$ given by

$$\begin{aligned}\hat{H}^U &= \hat{U}^\dagger(t)\hat{H}\hat{U}(t) - i\hat{U}^\dagger(t)\frac{\partial\hat{U}(t)}{\partial t}\\ &= \omega_0\hat{N} + \omega_1\Delta\hat{n} + \omega_2\hat{N}\Delta\hat{n} + \frac{1}{4}(\gamma_a+\gamma_b+2\gamma_{ab})\hat{N}^2\\ &\quad -g\left(\hat{a}^\dagger\hat{b} + \hat{a}\hat{b}^\dagger\right) + \frac{1}{4}(\gamma_a+\gamma_b-2\gamma_{ab})\Delta\hat{n}^2. \quad (4)\end{aligned}$$

Here, we define $\omega_0 = (\tilde{\omega}_a + \tilde{\omega}_b)/2$, $\omega_1 = (\tilde{\omega}_a - \tilde{\omega}_b - \Delta)/2$, and $\omega_2 = (\gamma_a - \gamma_b)/2$. $\hat{N} = \hat{n}_a + \hat{n}_b$ is the number operator, which accounts for the total number of bosons in the system and $\Delta\hat{n} = \hat{n}_a - \hat{n}_b$. However, because N is a conserved quantity, it will work as a c-number.

The Hamiltonian is nonlinear because the last term depends on the $\Delta\hat{n}^2$ operator. Defining a new parameter Λ as

$$\Lambda = \frac{1}{4}(\gamma_a + \gamma_b - 2\gamma_{ab}), \quad (5)$$

we note that the system becomes linear if $\Lambda = 0$, a condition that is valid for rubidium collisions [19, 20]. For this case, the transformed Hamiltonian becomes

$$\hat{H}^U = \omega_0\hat{N} + \omega_1\Delta\hat{n} + \omega_2\hat{N}\Delta\hat{n} + \gamma_{ab}\hat{N}^2 - g\left(\hat{a}^\dagger\hat{b} + \hat{a}\hat{b}^\dagger\right). \quad (6)$$

Henceforth, we will call Λ the *linearity parameter* as (5) is the necessary condition for obtaining the effective Hamiltonian (6). In the case of rubidium collisions, it applies that $\Lambda = 0$ [19, 20], although the manipulation of this parameter is possible using Feshbach resonances, which affect collisions between atoms from different hyperfine levels [15, 24].

The second transformation

$$\hat{V} = e^{\frac{\xi}{2}\left(\hat{a}^\dagger\hat{b} - \hat{a}\hat{b}^\dagger\right)},$$

being ξ an arbitrary parameter, is used to obtain a diagonal transformed Hamiltonian $\hat{H}^V = \hat{V}^\dagger\hat{H}^U\hat{V}$. After some algebra, we find that

$$\begin{aligned}\hat{H}^V &= \omega_0\hat{N} + \gamma_{ab}\hat{N}^2 + \left[\left(\omega_1 + \omega_2\hat{N}\right)\cos\xi + g\sin\xi\right]\Delta\hat{n}\\ &\quad + \left[\left(\omega_1 + \omega_2\hat{N}\right)\sin\xi - g\cos\xi\right]\left(\hat{a}^\dagger\hat{b} + \hat{a}\hat{b}^\dagger\right).\end{aligned}$$

If ξ fulfills the condition

$$\xi = \arctan\left(\frac{g}{\omega_1 + \omega_2 N}\right),$$

the above Hamiltonian becomes

$$\hat{H}^V = \omega_0\hat{N} + \gamma_{ab}\hat{N}^2 + \left(\omega_1'\cos\xi + g\sin\xi\right)\Delta\hat{n}. \quad (7)$$

After all of these considerations, we obtain the final form for the evolved state (3), which reads as

$$|\Psi(t)\rangle = \hat{U}(t)\hat{V}e^{-\iota\hat{H}^V t}\hat{V}^\dagger|\Psi(0)\rangle.$$

This means that $\hat{P}(t)$ is given by

$$\hat{P}(t) = \hat{U}(t)\hat{V}e^{-\iota\hat{H}^V t}\hat{V}^\dagger. \quad (8)$$

Now, we proceed to demonstrate how the evolution operator is a product of rotation operators by using the connection between two quantum harmonic oscillators and pseudo-spin operators [31]. This connection enables the pseudo-spin boson operators to be written as $\hat{J}_x = \hat{a}^\dagger\hat{b} + \hat{a}\hat{b}^\dagger$, $\hat{J}_y = -i\left(\hat{a}^\dagger\hat{b} - \hat{a}\hat{b}^\dagger\right)$, and $\hat{J}_z = \hat{a}^\dagger\hat{a} - \hat{b}^\dagger\hat{b}$. In this way, the operator $\hat{P}(t)$ takes the form

$$\hat{P}(t) = e^{-\iota\eta t}e^{-\iota\frac{\Delta}{2}t\hat{J}_z}e^{\iota\frac{\xi}{2}\hat{J}_y}e^{-\iota\frac{\varpi}{2}\hat{J}_z t}e^{-\iota\frac{\xi}{2}\hat{J}_y}. \quad (9)$$

The operators inside the general expression above are, in fact, rotation operators [28, 31] because the operators $\hat{J}_i$ $(i = x, y, z)$ are generators of rotations around the ith axis. The final form of $\hat{P}(t)$ as a function of rotation operators $\hat{R}_i$ is

$$\hat{P}(\eta, \Delta, \varpi, \xi, t) = e^{-\iota\eta t}R_z(\Delta t)R_y(-\xi)R_z(\varpi t)R_y(\xi), \quad (10)$$

where the auxiliary parameters are defined as

$$\begin{aligned}\xi &= \arctan\left(\frac{2g}{\Gamma - \Delta}\right),\\ \varpi &= (\Gamma - \Delta)\cos\xi + 2g\sin\xi,\\ \eta &= \frac{1}{2}\left[(\omega_a + \omega_b) + (\gamma_a + \gamma_b)(N-1)\right]N. \quad (11)\end{aligned}$$

Here, we define the *frequency-scattering detuning* as

$$\Gamma = \omega_{ab} + (\gamma_a - \gamma_b)(N-1), \quad (12)$$

where $\omega_{ab} = \omega_a - \omega_b$ is the detuning between the effective trap frequency for each condensate. The parameter Γ quantifies differences between the trap frequencies and collision parameters on each condensate. This quantity and the linearity parameter, Λ, play important roles in defining the necessary conditions for the implementation of quantum logic gates.

After obtaining the evolution operator defined above, we proceed to exploit the possibilities of applying coupled Bose-Einstein condensates (CBECs) within the context of quantum information processing. In the following section, we encode a qubit using CBECs and explore the behavior of

the operator (10) for the implementation of quantum logic gates.

3 Single-Qubit Codification and Quantum Logic Operations

In the standard quantum computation approach, encoding information requires the preparation of an initial state, which is defined on a computational basis $\{|0\rangle, |1\rangle\}$ as a coherent superposition with coefficients α and β. Definitions of qubits using CBECs are found in the literature, particularly in the context of condensed atoms in a two-site potential [10]. Our proposal is to encode the qubit using an atomic coherent state (ACS) [3], which can be created with hyperfine CBECs following the application of a $\pi/2$ pulse [17, 30]. The ACS is defined as

$$\begin{aligned} |\theta,\phi\rangle &= \frac{1}{\sqrt{N!}}\left[\cos\left(\frac{\theta}{2}\right)a^{\dagger} + \sin\left(\frac{\theta}{2}\right)e^{\imath\phi}b^{\dagger}\right]^{N}|0,0\rangle, \\ &= e^{\theta\left(\cos\phi\hat{J}_x+\sin\phi\hat{J}_y\right)}\left|\frac{N}{2},-\frac{N}{2}\right\rangle, \end{aligned} \tag{13}$$

where θ is related to the difference between the atomic populations of hyperfine levels and ϕ gives the relative phase between them. The state (13) describes a particle with spin $N/2$, whose normalized mean values of the operators are given by $< Jx > /N = \sin\theta\cos\phi$, $< Jy > /N = \sin\theta\sin\phi$, and $< Jz > /N = \cos\theta$. ACS is analogous to the coherent state of the harmonic oscillator: it is the result of applying a displacement operation over the ground state $|N/2, -N/2\rangle = |1\rangle$ and is a minimum uncertainty state that fulfills the Heisenberg angular-momentum uncertainty relation

$$\left\langle(\Delta J_{x'})^2\right\rangle\left\langle\left(\Delta J_{y'}\right)^2\right\rangle \geq \frac{1}{4}\left|\langle J_{z'}\rangle\right|^2,$$

where the mean values are calculated in a rotated coordinate system; thus, z' is an axis that passes through the center of the ACS [13]. This state can be represented on a Bloch sphere by

$$|\theta,\phi\rangle = \cos\frac{\theta}{2}|0\rangle + \sin\frac{\theta}{2}e^{i\phi}|1\rangle = \alpha|0\rangle + \beta|1\rangle, \tag{14}$$

where $|0\rangle = |0, N\rangle$ and $|1\rangle = |N, 0\rangle$, with θ and ϕ being the polar and azimuthal angles on the Bloch sphere, respectively. The relation between (13) and (14) allows us to map an ACS as a qubit.

Notably, under the action of $\hat{P}(t)$, (10), the ACS evolves to another ACS with new coefficients $\alpha(t)$ and $\beta(t)$. This is because the evolution operator is a succession of rotations, which preserve the condition of the minimum uncertainty state. To find the experimental conditions for implementing single-qubit quantum gates, we use the 2×2 matrix representation of rotation operators R_z and R_y [28]. Through the map given by (14) and using the relation between pseudo-spin operators and rotations, we obtain the matrix form of $\hat{P}$, given by

$$\hat{P}(\eta,\Delta,\varpi,\xi,t) \to e^{-\imath\eta t}\begin{pmatrix} P_{11} & P_{12} \\ P_{21} & P_{22}\end{pmatrix}, \tag{15}$$

where

$$\begin{aligned} P_{11} &= e^{-\imath\frac{\Delta t}{2}}e^{-\imath\frac{\varpi}{2}t}\left(\cos^2\frac{\xi}{2} + e^{\imath\varpi t}\sin^2\frac{\xi}{2}\right) \\ P_{12} &= 2\imath\cos\frac{\xi}{2}\sin\frac{\xi}{2}\sin\left(\frac{\varpi}{2}t\right)e^{-\imath\frac{\Delta t}{2}} \\ P_{21} &= 2\imath\cos\frac{\xi}{2}\sin\frac{\xi}{2}\sin\left(\frac{\varpi t}{2}\right)e^{\imath\frac{\Delta t}{2}} \\ P_{22} &= e^{\imath\frac{\Delta t}{2}}e^{-\imath\frac{\varpi t}{2}}\left(\sin^2\frac{\xi}{2} + e^{\imath\varpi t}\cos^2\frac{\xi}{2}\right). \end{aligned} \tag{16}$$

We are now able to find the necessary conditions for the realization of a specific single-qubit gate. In the particular context of coupled BECs, this operation can be sorted into two sets depending on the type of dynamics required for each gate. The first set, the *population-transfer* gates, contains the NOT, Y, and Hadamard gates and requires population transfer as well as changes in the relative phase between the coupled condensates. From a geometrical perspective, the evolution operator $\hat{P}(t)$ will change the polar angle and azimuthal angle of the qubit on the Bloch sphere. The second set, the *phase* gates, given by the Z, S, and T gates, requires self-trapping [23, 32], meaning the inhibition of population transfer, together with the change of relative phase.

For the first set, it is useful to recall the matrix forms of gates NOT, $\hat{Y}$, and $\hat{H}$, which are written as

$$\hat{X} \equiv \begin{pmatrix} 0 & 1 \\ 1 & 0\end{pmatrix}, \quad \hat{Y} \equiv \begin{pmatrix} 0 & -i \\ i & 0\end{pmatrix}, \quad \hat{H} \equiv \frac{1}{\sqrt{2}}\begin{pmatrix} 1 & 1 \\ 1 & -1\end{pmatrix}, \tag{17}$$

while the phase gates ($\hat{G}_p$) are given by the general expression

$$\hat{G}_p = \begin{pmatrix} 1 & 0 \\ 0 & e^{i\varphi}\end{pmatrix}, \tag{18}$$

with the value of the relative phase φ corresponding to $\hat{G}_P = \hat{Z}$ ($\varphi = \pi$), $\hat{S}$ ($\varphi = \pi/2$), and $\hat{T}$ ($\varphi = \pi/4$) quantum gates, respectively.

To obtain the conditions for physical implementation, we proceed to compare each matrix element of the evolution operator $\hat{P}$ with the corresponding elements of (17) and (18). Let us consider the NOT quantum gate, $\hat{X}$ in (17). Comparing both the matrix form for this gate and (15), the elements of P must be given by $P_{11} = P_{22} = 0$ and $P_{12} = P_{21} = 1$. After some algebra, we found that the detuning must follow the rule $\Delta = \frac{2\pi}{t}$. During experiments, it is possible to control the two-photon detuning, Δ; thus, we fix the gate evolution

time as $t_{\mathrm{NOT}} = \frac{2\pi}{\Delta}$. Moreover, the values of the auxiliary parameters defined in (11) must fulfill the following conditions

$$\begin{aligned} \xi &= \arctan\left(\frac{2g}{\Gamma-\Delta}\right) \equiv \frac{\pi}{2}, \\ \varpi &= (\Gamma-\Delta)\cos\xi + 2g\sin\xi \equiv \frac{\Delta}{2}, \\ \eta &= \frac{1}{2}\left[(\omega_a+\omega_b)+(\gamma_a+\gamma_b)(N-1)\right]N \equiv \frac{3\Delta}{8}. \end{aligned} \tag{19}$$

The solution of this coupled equation defines two physical requirements: first, the value of the two-photon transition, Δ, must be set as $\Delta = \Delta_{\mathrm{G}} = 4g$. Second, the frequency-scattering detuning, Γ, given by (12), must follow the condition $\Gamma = \Gamma_{\mathrm{G}} = 4g$.

Following a similar procedure, we found the values for t_{gate}, Δ_{G}, and Γ_{G} for all population-transfer gates, which are summarized in Table 1. We note that the detuning of the two-photon transition, Δ_{G}, depends on the coupling parameter g with the rule $\Delta_{\mathrm{G}} = n^{\mathrm{G}}g$, with n^{G} being a different factor for each gate. The operation time is also a function of the coupling parameter g, which is responsible for the population transfer, and all gates require a non-resonant two-photon coupling and specific non-zero values of the Γ_{G} parameter. This is because these two parameters (Δ_{G} and Γ_{G}) control the gain of relative phase between $|0\rangle$ and $|1\rangle$. For CBECs on a chip [4], it is possible to control ω_{ab} while $\gamma_a - \gamma_b$ is a fixed value. However, in the experimental setup of Gross et al. [17], the values of the collision parameters γ_i can be manipulated via Feschbach resonances, leaving ω_{ab} fixed.

Regarding the phase gates, operators $\hat{G}_p$, where the goal is to obtain a relative phase suppressing the population transfer, we expect that the requirements for the implementation of this gate include a detuned two-photon transition.

Table 1 Evolution times and necessary conditions for the implementation of the population-transfer gates given by NOT, $\hat{Y}$, and $\hat{H}$

Gate	t_{gate}	Δ_{G}	Γ_{G}
NOT	$\frac{2\pi}{\Delta}$	$4g$	$4g$
$\hat{Y}$	$\frac{\pi}{\Delta}$	$2g$	$2g$
$\hat{H}$	$\frac{2\pi}{\Delta}$	$\frac{8}{\sqrt{2}}g$	$-2g+\Delta$

Here, g is the coupling parameter, Δ_{G} is the detuning of the two-photon coupling, and Γ_{G} is the frequency-scattering detuning, as defined in (12)

Let us begin our analysis with the gate $\hat{Z}$, which is written as

$$\hat{Z} = \begin{pmatrix} 1 & 0 \\ 0 & -1 \end{pmatrix}.$$

Comparing this matrix with the general expressions for the matrix elements of $\hat{P}$, (16), we obtain that the time evolution of the gate is $t_Z = \pi/2\Delta$, and, after some algebra, we also found the conditions for the auxiliary parameters, which are

$$\begin{aligned} \xi &= \arctan\left(\frac{2g}{\Gamma-\Delta}\right) \equiv \pi, \\ \varpi &= (\Gamma-\Delta)\cos\xi + 2g\sin\xi \equiv 3\Delta, \\ \eta &= \frac{1}{2}\left[(\omega_a+\omega_b)-(\gamma_a+\gamma_b)\right]N + \gamma_{ab}N^2 \equiv \Delta. \end{aligned} \tag{20}$$

These equations have two possible mathematical solutions: the first one is considering $g = 0$, which is not interesting because it describes uncoupled condensates. The second solution is obtained when $\Delta = \Delta_{\mathrm{G}} \gg 2g/3$, which implies a strong detuning of the two-photon transition, as expected. This requirement for detuning Δ_{G} is responsible for self-trapping. For $\hat{S}$ and $\hat{T}$, we obtain a similar condition for Δ_{G}, and, because the value of Δ_{G} is fixed, a careful setting of the quantity $\Gamma = \Gamma_{\mathrm{G}}$ is required to obtain the correct phase gain. With this consideration, we obtain the conditions for the implementation of all phase gates that are summarized in Table 2.

It is interesting to analyze the behavior of our system under the action of the gates by calculating the mean values of the operators $\hat{J}_i$ ($i = x, y, z$). The mean values are calculated over the evolved state $|\Psi(t)\rangle$, obtaining:

$$\frac{\langle \hat{J}_i(t)\rangle}{N} = \cos\phi\sin\theta f_{1i} - \sin\phi\sin\theta f_{2i} + \cos\theta f_{3i}, \tag{21}$$

Table 2 Evolution times and necessary conditions for the implementation of the quantum phase gates ($\hat{Z}$, $\hat{S}$, and $\hat{T}$)

Gate	t_{gate}	Δ_{G}	Γ_{G}
$\hat{Z}$	$\frac{\pi}{2\Delta}$	$\gg \frac{2g}{3}$	-2Δ
$\hat{S}$	$\frac{3\pi}{2\Delta}$	$\gg 3g$	$\frac{\Delta}{3}$
$\hat{T}$	$\frac{\pi}{2\Delta}$	$\gg 4g$	$\frac{\Delta}{2}$

Here, g is the coupling parameter, Δ_{G} is the detuning of the two-photon coupling, and Γ_{G} is the frequency-scattering detuning, as defined in (12)

where we defined the auxiliary functions f_{ki} ($k = 1, 2, 3$ and $i = x, y, z$) as

$$\begin{aligned}
f_{1x} &= \cos(\Delta t)\left[\cos^2(\xi)\cos(\varpi t) + \sin^2(\xi)\right] \\
&\quad - \sin(\Delta t)\sin(\varpi t)\cos(\xi), \\
f_{2x} &= \cos(\Delta t)\cos(\xi)\sin(\varpi t) + \sin(\Delta t)\cos(\varpi t), \\
f_{3x} &= \cos(\Delta t)\cos(\xi)\sin(\xi)[\cos(\varpi t) - 1] \\
&\quad - \sin(\Delta t)\sin(\varpi t)\sin(\xi) \\
f_{1y} &= \sin(\Delta t)\left[\cos^2(\xi)\cos(\varpi t) + \sin^2(\xi)\right] \\
&\quad + \cos(\Delta t)\cos(\xi)\sin(\varpi t), \\
f_{2y} &= \cos(\Delta t)\cos(\varpi t) - \sin(\Delta t)\sin(\varpi t)\cos(\xi), \\
f_{3y} &= \sin(\Delta t)[\cos(\varpi t)\sin(\xi)\cos(\xi) - \cos(\xi)\sin(\xi)] \\
&\quad + \cos(\Delta t)\sin(\varpi t)\sin(\xi), \\
f_{1z} &= \cos(\varpi t)\sin(\xi)\cos(\xi) - \sin(\xi)\cos(\xi), \\
f_{2z} &= \sin(\varpi t)\sin\xi, \\
f_{3z} &= \cos^2(\xi) + \cos(\varpi t)\sin^2(\xi).
\end{aligned} \tag{22}$$

In Fig. 1, we plot the evolution over the Bloch sphere of the vector with components defined as

$$(x, y, z) \rightarrow \left(\frac{\langle \hat{J}_x \rangle}{N}, \frac{\langle \hat{J}_y \rangle}{N}, \frac{\langle \hat{J}_z \rangle}{N}\right). \tag{23}$$

The initial state in (3) is given by $|\Psi(0)\rangle = \alpha|0\rangle + \beta|1\rangle$, with $\alpha = \cos\left(\frac{3\pi}{16}\right)$ and $\beta = \sin\left(\frac{3\pi}{16}\right)$. We consider the conditions for the implementation of gates NOT in Fig. 1a and $\hat{Y}$ in Fig. 1b. The phase gates are also shown, where $\hat{Z}$ corresponds to Fig. 1c and $\hat{S}$ is plotted in Fig. 1d. We note that the initial state $|\Psi(0)\rangle = \alpha|0\rangle + \beta|1\rangle$ evolves to a final state in agreement with the action of each quantum gate operation: $|\Psi(t_{\text{NOT}})\rangle = \alpha|1\rangle + \beta|0\rangle$ for the NOT operation shown in Fig. 1a, $|\Psi(t_{\text{Y}})\rangle = \alpha|1\rangle - \beta|0\rangle$ for the Y operation in Fig. 1b, $|\Psi(t_{\text{Z}})\rangle = \alpha|0\rangle - \beta|1\rangle$ for the Z operation in Fig. 1c and $|\Psi(t_{\text{S}})\rangle = \alpha|0\rangle + i\beta|1\rangle$ for the S operation in Fig. 1d. In Fig. 2, we show the action of the $\hat{H}$ gate by analyzing the evolution of the Bloch vector (23) considering four initial conditions. This gate acts over the states of the computational basis to create a superposition with a relative

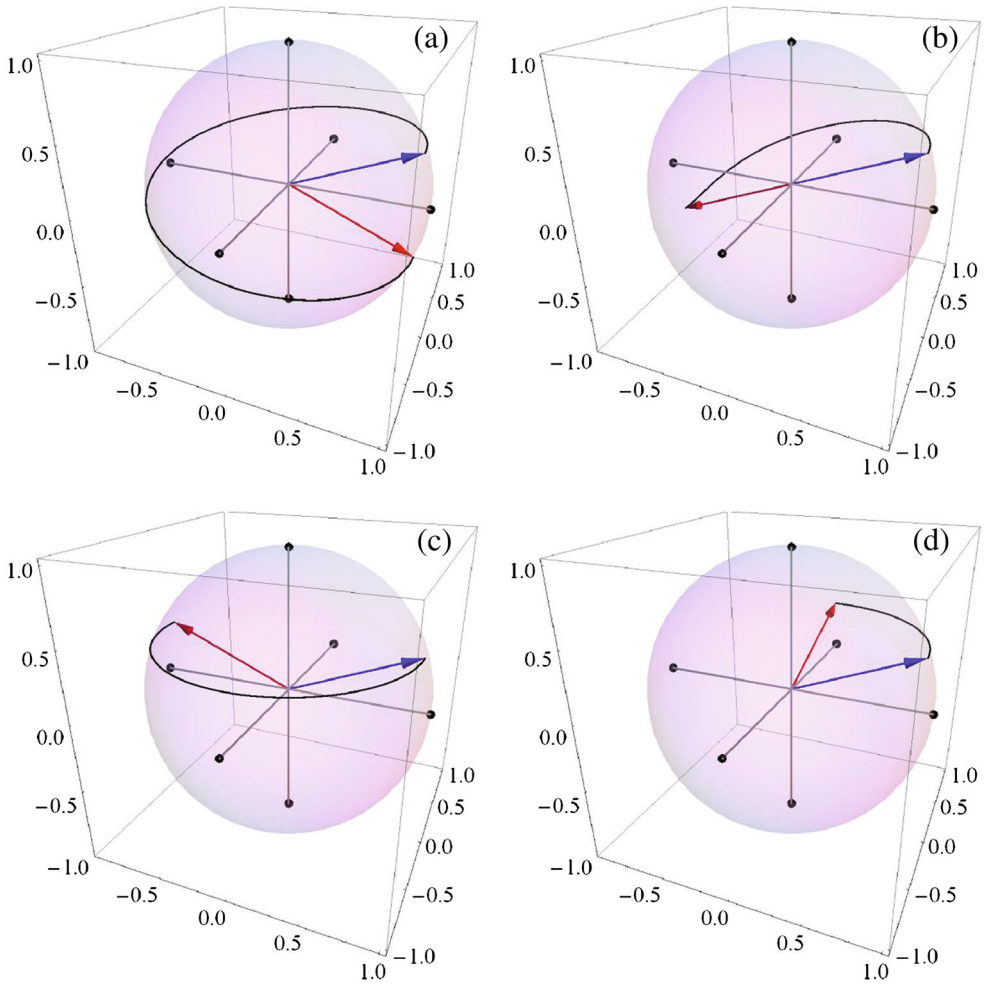

Fig. 1 Dynamics over the Bloch state considering the initial state $|\Psi(0)\rangle = \alpha|0\rangle + \beta|1\rangle$ under the action of **a** NOT, **b** $\hat{Y}$, **c** $\hat{Z}$, and **d** $\hat{S}$ gates. The *blue arrow* denotes the initial state, while the red one denotes the final state

phase of 0 (plus signal) and π (minus signal). The states $|0\rangle$ and $|1\rangle$, which are used to create the superpositions $\frac{|0\rangle+|1\rangle}{\sqrt{2}}$ and $\frac{|0\rangle-|1\rangle}{\sqrt{2}}$, are shown in Fig. 2a, b, respectively. The same gate takes the last superpositions to the original states, as shown in Fig. 2c, d.

From these results, our expectation is that the guidance provided by Tables 1 and 2, together with a careful manipulation of the physical parameters on coupled BECs, becomes a practical path to follow for the implementation of all single-qubit quantum gates. In the next section, we present a discussion on the experimental feasibility, including a study on the robustness against errors on settings outside of the ideal conditions for implementing the gates discussed above.

4 Experimental Feasibility

Regarding the feasibility of our proposal, the first task is to compare the evolution times for the quantum gates with the time scale of the typical decoherence processes for BECs. Let us consider the value of the coupling parameter for the experimental setup of an atomic chip [4] to calculate the evolution time t_{gate} for each gate. To estimate the value of coupling g, we use the reported value of $t_{\pi/2} = 170$ μs [4] associated with the application of a $\pi/2$ pulse, which means that the two-photon coupling is $g = 2\pi \times \frac{1}{4t_{\pi/2}} \cong 2\pi \times 1.5$ kHz. Using Table 1, we find that the evolution times associated with NOT, $\hat{Y}$, and $\hat{H}$ gates are given by $t_{\text{NOT}} = t_{\hat{Y}} = 0.16$ ms and $t_{\hat{H}} = 0.12$ ms, respectively. These values are significantly lower than the decoherence time, with a value of approximately 3 s [36]. For the experimental setup of Gross et al. [17], the value of the coupling parameter can be switched between zero and $g = 2\pi \times 600$ Hz. Considering the highest value of g, we found that the time scales for the gates are $t_{\text{NOT}} = t_{\hat{Y}} = 0.42$ ms and $t_{\hat{H}} = 0.29$ ms, which is 10^{-4} times the decoherence time. Because the phase gates require a detuned interaction ($\Delta_{\text{G}} \gg g$), the time scale goes as $t_{\text{gate}} \propto 1/\Delta_{\text{G}}$.

The second and third tasks consist of checking the effects of nonlinearity ($\Lambda \neq 0$) and the sensitivity of the dynamics against changes in the values of frequency-

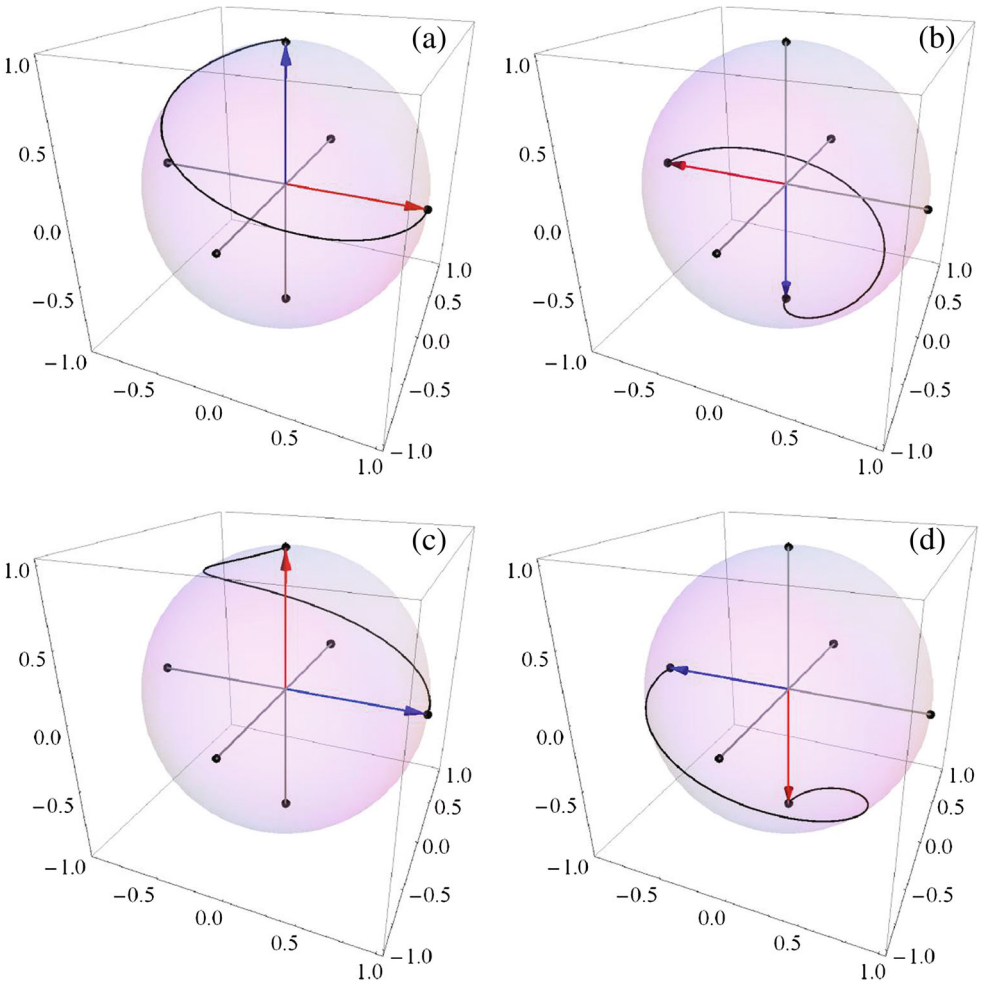

Fig. 2 Dynamics under the action of the Hadamard gate for initial states given by **a** $|0\rangle$, **b** $|1\rangle$, **c** $\frac{|0\rangle+|1\rangle}{\sqrt{2}}$, and **d** $\frac{|0\rangle-|1\rangle}{\sqrt{2}}$

scattering detuning, Γ, and the two-photon detuning, Δ_G, as defined in Tables 1 and 2. Hao and Gu [22] studied the dynamics associated with Hamiltonian (1), considering non-zero values for nonlinear conditions. The nonlinearity, which depends on $\hat{J}_z^2$, would affect our qubit because the ACS becomes a squeezed state [16] as time increases. This coupling also induces self-trapping, which might reduce the fidelity of quantum gates NOT, $\hat{Y}$, and $\hat{H}$. Changes in the specific conditions for Γ and Δ_G could affect the fidelity of the implementation of quantum gates because they are crucial for both the necessary gain of relative phase and transfer of population.

To quantify the robustness of the gates, we perform simulations with the goal of solving the Schrödinger equation to calculate the exact state $|\Psi(t_{\text{gate}})\rangle$. We compare the match between the target gate state, $|\Psi_{\text{gate}}\rangle$, and $|\Psi(t_{\text{gate}})\rangle$, calculating the fidelity defined as

$$\mathcal{F} = \left|\langle\Psi_{\text{gate}}|\Psi(t_{\text{gate}})\rangle\right|^2. \tag{24}$$

For our simulations, we consider $N = 1000$, the initial state being $|\theta, \phi\rangle = |\pi/8, 0\rangle$, and values for physical parameters according to experimental setup of C. Gross et al. [17]. To quantify the effects of nonlinearity, we perform numerical simulations by increasing the value of γ_{ab} to obtain $\Lambda \neq 0$. Using a similar procedure, we quantify the effects of the Γ parameter defined for each gate in Tables 1 and 2, consider increasing values of ω_{ab} such that $\Delta\Gamma = |\Gamma_s - \Gamma_G| \neq 0$, where Γ_s is the value used in the simulation and Γ_G is the value in Tables 1 and 2. The effect of changes on the Δ condition is quantified by considering $\delta\Delta = |\Delta_s - \Delta_G|$, where Δ_s is the value used in simulation.

In Fig. 3, we plot our results of fidelity as a function of both Λ and $\Delta\Gamma/\Gamma$, considering four gates: (a) $\hat{H}$, (b) $\hat{X}$ and $\hat{Y}$, (c) $\hat{S}$, and (d) $\hat{Z}$. For population-transfer gates, it is observed that the exact conditions for Λ and Γ_G obtained by analytical calculations are not exclusive for the implementation of a gate with high fidelity: the dark region with $F = 1$ extends to several choices for Λ and $\Delta\Gamma/\Gamma$, with a linear relation between the two parameters for the Hadamard gate, as shown in Fig. 3a, and a less extended region for $\hat{X}$ and $\hat{Y}$ gates, as shown in Fig. 3b. These two behaviors are understood through the definition for the Γ parameter, (12): because this quantity depends on the collision parameter γ_i, for small values of Λ, the effect of nonlinearity can be compensated by modifying the frequency-scattering detuning, which provides an extended set of experimental values with high fidelity gates. In the case of phase gates, the effect of $\Delta\Gamma$ over the decay of fidelity is weaker than the effect of the nonlinearity parameter. This is explained by the fact that phase gates do not require a specific value of two-photon detuning, and thus, setting this parameter as significantly higher than the coupling parameter g is sufficient. Because the condition for Γ_G depends directly on Δ, the variations around the ideal value of Γ_G in Table 2 do not significantly affect the fidelity of the gates.

The final issue is to quantify the robustness of population-transfer gates out of the specific condition for detuning Δ_G defined in Table 1. In Fig. 4, we present our numerical results for the three population-transfer gates. From these results, we observe that the fidelity for all gates drastically decreases when $\delta\Delta$ increases. Nevertheless, all three cases have the same behavior for small changes of Δ; thus, $\delta\Delta/\Delta_G \leq 0.1$. For this interval of values, the fidelity has high values with $F > 0.8$, as indicated by the black dash line in Fig. 4. Additionally, the Hadamard and the $\hat{Y}$ gates continue with equal behavior until $\delta\Delta/\Delta_G = 0.17$, with $F > 0.6$. After that value, the fidelity of the $\hat{X}$ gate has slower decay than that of the other two gates. The last gates have the same behavior until $\delta\Delta/\Delta_G = 0.15$ (gray dash line in Fig. 4), with the Hadamard gate being the least robust gate against small changes in the detuning value. From our simulations, we can conclude that fluctuations below

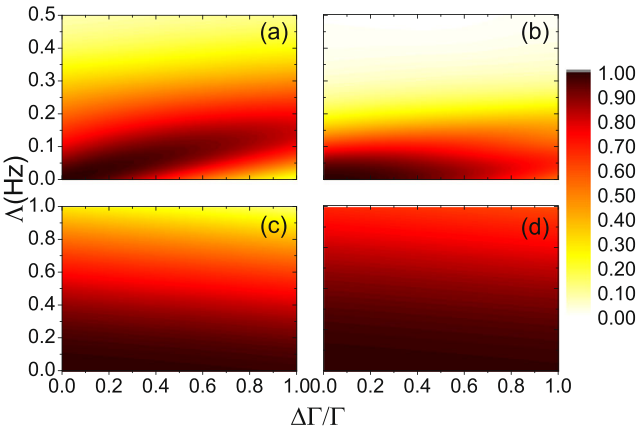

Fig. 3 Fidelity of **a** $\hat{H}$, **b** $\hat{X}$, **c** $\hat{S}$, and **d** $\hat{Z}$ gates as a function of Λ and $\Delta\Gamma/\Gamma$

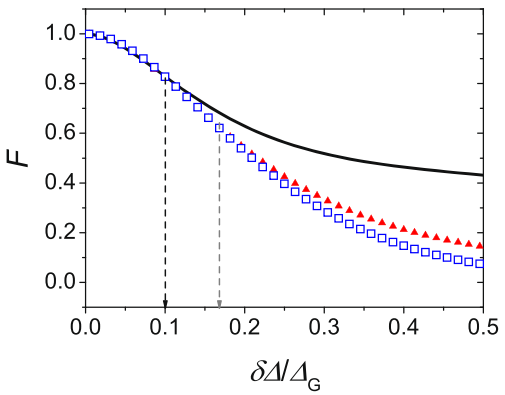

Fig. 4 Fidelity behavior for $\hat{X}$ (*black solid line*), $\hat{Y}$ (*red triangles*), and $\hat{H}$ (*blue open squares*) gates as a function of Δ_G

10 % can be considered small because they are associated with high values of fidelity. Thus, a careful manipulation of the two-photon detuning is mandatory, particularly for the implementation of $\hat{Y}$ and $\hat{H}$ gates, once this parameter affects not only the relative phase of the final state but also the transfer of population.

5 Summary

In this work, we explore the properties of coupled Bose-Einstein condensates with the specific goal of implementing controlled single-qubit quantum gates. Our system consists of atoms condensed in two different hyperfine levels interacting via two-body collisions and coupled by a two-photon transition. We solve the Schrödinger equation to explore the dynamics and obtain the necessary physical conditions for implementing two sets of gates: those that require a population transfer (NOT, $\hat{Y}$ and $\hat{H}$) and the phase gates. We check the behavior of a Bloch vector defined using the mean values of pseudo-spin operators $\hat{J}_i$, with $i = x, y, z$ setting the necessary conditions for each quantum logic gate. We conclude that the careful experimental control over the different detunings of the system (Δ, $\omega_a - \omega_b$ and $\gamma_a - \gamma_b$) leads to the implementation of high fidelity quantum gates. The feasibility of our proposal was explored through numerical simulations, considering the effects of nonlinearity and deviations from the required value for the frequency-scattering condition, Γ_G, as well as the two-photon detuning Δ_G. Our results show that it is possible to implement gates with high fidelity outside of the ideal conditions, respecting the limiting values obtained in Section 4.

Acknowledgmens This work was supported by the Brazilian National Institute of Science and Technology for Quantum Information (INCT-IQ), grant number 573658/2008-0, CAPES, grant number 552338/2011-7, FAPEMIG, grant number APQ-01768-14, and CNPq, grant number 552338/2011-7.

References

1. M. Albiez, R. Gati, J. Fölling, S. Hunsmann, M. Cristiani, M.K. Oberthaler, Direct observation of tunneling and nonlinear self-trapping in a single Bosonic Josephson junction. Phys. Rev. Lett. **95**, 010402 (2005)
2. M.H. Anderson, J.R. Ensher, M.R. Matthews, C.E. Wieman, E.A. Cornell, Observation of Bose-Einstein condensation in a dilute atomic vapor. Science **269**(5221), 198 (1995)
3. F.T. Arecchi, E. Courtens, R. Gilmore, H. Thomas, Atomic coherent states in quantum optics. Phys. Rev. A **6**, 2211 (1972)
4. P. Böhi, M.F. Riedel, J. Hoffrogge, J. Reichel, T.W. Haensch, P. Treutlein, Coherent manipulation of Bose-Einstein condensates with state-dependent microwave potentials on an atom chip. Nat. Phys. **5**, 592 (2009)
5. T. Byrnes, K. Wen, Y. Yamamoto, Macroscopic quantum computation using Bose-Einstein condensates. Phys. Rev. A **85**, 040306 (2012)
6. T. Calarco, E.A. Hinds, D. Jaksch, J. Schmiedmayer, J.I. Cirac, P. Zoller, Quantum gates with neutral atoms: controlling collisional interactions in time-dependent traps. Phys. Rev. A **61**, 022304 (2000)
7. T. Calarco, D. Jaksch, J.I. Cirac, P. Zoller, Controlling dynamical phases in quantum optics. J. Opt. B: Quantum Semiclassical Opt. **4**(4), S430 (2002)
8. T. Calarco, U. Dorner, P.S. Julienne, C.J. Williams, P. Zoller, Quantum computations with atoms in optical lattices: Marker qubits and molecular interactions. Phys. Rev. A **70**, 012306 (2004)
9. F.S. Cataliotti, S. Burger, C. Fort, P. Maddaloni, F. Minardi, A. Trombettoni, A. Smerzi, M. Inguscio, Josephson junction arrays with Bose-Einstein condensates. Science **293**(5531), 843 (2001)
10. Z.B. Chen, Y.D. Zhang, Possible realization of Josephson charge qubits in two coupled Bose-Einstein condensates. Phys. Rev. A **65**, 022318 (2002)
11. J. Cirac, M. Lewenstein, K. Mølner, P. Zoller, Quantum superposition states of Bose-Einstein condensates. Phys. Rev. A **57**, 1208–1218 (1998)
12. K.B. Davis, M.O. Mewes, M.R. Andrews, N.J. Van Druten, D.S. Durfee, D.M. Kurn, W. Ketterle, Bose-Einstein condensation in a gas of Sodium atoms. Phys. Rev. Lett. **75**, 3969–3973 (1995)
13. J.P. Dowling, G.S. Agarwal, W.P. Schleich, Wigner distribution of a general angular-momentum state: applications to a collection of two-level atoms. Phys. Rev. A **49**, 4101 (1994)
14. E.I. Duzzioni, L. Sanz, S.S. Mizrahi, M.H.Y. Moussa, Control of the geometric phase and pseudospin dynamics on coupled Bose-Einstein condensates. Phys. Rev. A **75**, 032113 (2007)
15. M. Erhard, H. Schmaljohann, J. Kronjaäger, K. Bongs, K. Sengstock, Measurement of a mixed-spin-channel Feshbach resonance in ^{87}rb. Phys. Rev. A **69**, 032705 (2004)
16. J. Estève, C. Gross, A. Weller, S. Giovanazzi, M. Oberthaler, Squeezing and entanglement in a Bose-Einstein condensate. Nature **455**, 1216 (2008)
17. C. Gross, T. Zibold, E. Nicklas, J. Estève, M. Oberthaler, Nonlinear atom interferometer surpasses classical precision limit. Nature **464**, 1165 (2010)
18. L.K. Grover, A fast quantum mechanical algorithm for database search. Phys. Rev. Lett. **79**, 325 (1997)
19. D.S. Hall, M.R. Matthews, J.R. Ensher, C.E. Wieman, E.A. Cornell, Dynamics of component separation in a binary mixture of Bose-Einstein condensates. Phys. Rev. Lett. **81**, 1539–1542 (1998a)
20. D.S. Hall, M.R. Matthews, C.E. Wieman, E.A. Cornell, Measurement of relative phase in two-component Bose-Einstein condensates. Phys. Rev. Lett. **81**, 1543–1546 (1998b)
21. W. Hänsel, P. Hommelhoff, T.W. Hänsch, J. Reichel, Bose-Einstein condensation on a microelectronic chip. Nature **413**, 498 (2001)
22. Y. Hao, Q. Gu, Dynamics of two-component Bose-Einstein condensates coupled with the environment. Phys. Rev. A **83**, 043620 (2011)
23. A.P. Hines, R.H. McKensie, G.J. Milburn, Entanglement of two-mode Bose-Einstein condensates. Phys. Rev. A **67**, 013609 (2003)
24. A.M. Kaufman, R.P. Anderson, T.M. Hanna, E. Tiesinga, P.S. Julienne, D.S. Hall, Radio-frequency dressing of multiple Feshbach resonance. Phys. Rev. A **80**, 050701(R) (2009)
25. T.D. Ladd, F. Jelezko, R. Laflamme, Y. Nakamura, C. Monroe, J.L. O'Brien, Quantum computers. Nature **464**, 45–53 (2010)

26. C. Lee, E.A. Ostrovskaya, Quantum computation with diatomic bits in optical lattices. Phys. Rev. A **72**, 062321 (2005)
27. G.J. Milburn, J. Corney, E.M. Wright, D.F. Walls, Quantum dynamics of an atomic Bose-Einstein condensate in a double-well potential. Phys. Rev. A **55**, 4318 (1997)
28. M.A. Nielsen, I.L. Chuang, Quantum Computation and Quantum Information (Cambridge University Press, Cambridge, 2000)
29. J.K. Pachos, P.L. Knight, Quantum computation with a one-dimensional optical lattice. Phys. Rev. Lett. **91**, 107902 (2003)
30. M.P. Riedel, P. Böhi, Y. Li, T.W. Hänsch, A. Sinatra, P. Treutlein, Atom-chip-based generation of entanglement for quantum metrology. Nature **464**, 1170–1173 (2010)
31. J. Sakurai, *Modern Quantum Mechanics*. Addison-Wesley, section 3.8, 217 (1994)
32. A.N. Salgueiro, A. de Toledo Piza, G.B. Lemos, R. Drumond, M.C. Nemes, M. Weidemüller, Quantum dynamics of bosons in a double-well potential: Josephson oscillations, self-trapping and ultralong tunneling times. Eur. Phys. J. D **44**(3), 537 (2007)
33. B. Schumacher, Quantum coding. Phys. Rev. A **51**, 2738 (1995)
34. P.W. Shor, *Proceedings of the 35th Annual Symposium of Computer Science* (IEEE Press, Los Alamitos, 1994)
35. M.J. Steel, M.J. Collett, Quantum state of two trapped Bose-Einstein condensates with a Josephson coupling. Phys. Rev. A **57**, 2920 (1998)
36. P. Treutlein, P. Hommelhoff, T. Steinmetz, T.W. Hänsch, J. Reichel, Coherence in microchip traps. Phys. Rev. Lett. **92**, 203005 (2004)
37. P. Villain, M. Lewenstein, Dephasing of Josephson oscillations between two coupled Bose-Einstein condensates. Phys. Rev. A **59**, 2250–2260 (1999)